

Simulation of the Ku-Band Radar Altimeter Sea Ice Effective Scattering Surface

Rasmus Tonboe, Søren Andersen, and Leif Toudal Pedersen

Abstract—A radiative transfer model is used to simulate the sea ice radar altimeter effective scattering surface variability as a function of snow depth and density. Under dry snow conditions without layering these are the primary snow parameters affecting the scattering surface variability. The model is initialized with *in situ* data collected during the May 2004 GreenIce ice camp in the Lincoln Sea (73°W; 85°N). Our results show that the snow cover is important for the effective scattering surface depth in sea ice and thus for the range measurement, ice freeboard, and ice thickness estimation.

Index Terms—Altimetry, modeling, sea ice, snow.

I. INTRODUCTION

THE backscatter coefficient for a space-borne altimeter system of snow-free, level sea ice is primarily a function of ice roughness and coherent surface scattering mechanisms within the snow/ice system [1]. Dielectric loss (attenuation) together with volume scattering determines the extinction of the propagating signal within snow and ice layers [2]. It has been suggested that backscatter at nadir angles of (dry) snow-covered sea ice is dominated by ice surface scattering [1], [3]. However, the link between the prominent scattering horizons and the effective scattering surface, when the altimeter is used for surface elevation measurements, is yet unclear. It is therefore the aim here to investigate, theoretically, the relation between the leading edge of the nadir looking radar pulse form and the sea ice snow cover and how the snow cover affects the altimeter effective scattering surface and thus of elevation or freeboard altimeter measurements.

Sea ice conditions even within a satellite altimeter resolution cell (CryoSat, about 250 × 7000 m) are often diverse. Our study is most realistically done over thick and large multiyear ice floes. These conditions are found in the Lincoln Sea where our *in situ* data are collected.

II. ALTIMETER WAVEFORM MODEL

The radiative transfer altimeter waveform model uses the physical snow and ice quantities and structure as input. In this model a sequence of layers is described by their density, exponential correlation length, thermometric temperature, and

Manuscript received May 30, 2005; revised August 26, 2005. This work was supported by the European Commissions 5th Framework Programme; GreenIce (EVK2-2001-00280).

R. Tonboe and S. Andersen are with the Danish Meteorological Institute, DK-2100 Copenhagen Ø, Denmark (e-mail: rtt@dmi.dk).

L. T. Pedersen is with Ørsted, Technical University of Denmark, DK-2800 Lyngby, Denmark.

Digital Object Identifier 10.1109/LGRS.2005.862276

TABLE I

MULTIYEAR ICE SNOW AND ICE PARAMETERS USED AS INPUT TO THE FORWARD MODEL, I.E., TEMPERATURE, T , FLAT-PATCH-AREA, F , DENSITY, ρ , LAYER THICKNESS, d , EXPONENTIAL CORRELATION LENGTH, p_{ec} . THE LAST COLUMN SHOWS THE COMPUTED PERMITTIVITY OF THE LAYERS, ϵ

layer	T [°C]	F [%]	ρ [kg/m ³]	d [m]	p_{ec} [mm]	ϵ
1 snow	-9.6	1.0	250	0.05	0.10	1.42+0.00i
2 snow	-9.1	0.0	250	0.05	0.10	1.42+0.00i
3 snow	-8.6	0.0	250	0.05	0.10	1.42+0.00i
4 snow	-8.0	0.0	250	0.05	0.10	1.42+0.00i
5 depth hoar	-7.4	0.0	250	0.05	0.25	1.42+0.00i
6 ice	-7.4	1.0	900	0.05	0.35	3.24+0.01i
7 ice	-7.3	0.0	900	0.20	0.35	3.24+0.01i
8 ice	-7.0 ... -3.0	0.0	900	3.30	0.25	3.34+0.04i ... 3.57+0.08i

the roughness here quantified as the fractional flat-patch-area, e.g., see [1] and [4]. The exponential correlation length is a measure of scatterer size and distribution, e.g., see [5]. Mixing formulas and empirical functions relate the physical snow and ice properties to the permittivity given in Table I [6]–[8]. The surface backscatter coefficient is computed using [1], i.e.,

$$\sigma_{\text{surf}} = 0.9F |R(0)|^2 \frac{H}{u\tau} \quad (1)$$

given by the pulse length, τ (3.125×10^{-9} s), the speed of light, u , the satellite height, H (800 km), the fractional flat-patch-area, F , and the nadir reflection coefficient, $R(0)$. This approach is found by [1] to be “more realistic” than the geometrical optics model. Yet the two models produce very similar results. The improved Born approximation, suitable for microwave scattering in snow [9], is used to compute the volume scattering coefficient (spherical inclusions) [10], i.e.,

$$\sigma_{\text{vol}} \cong \frac{3p_{ec}^3 k^4}{32} v(1-v) \left| \frac{(\epsilon_2 - \epsilon_1)(2\epsilon_{eff} + \epsilon_1)}{2\epsilon_{eff} + \epsilon_2} \right|^2 \quad (2)$$

where p_{ec} is the correlation length, k the wavenumber, v the volume fraction of scatterers and ϵ_1 , ϵ_2 , ϵ_{eff} are the permittivity of the background, the scatterers, and the layer, respectively. No specific correction is applied for antenna gain or pulse modulation in the characterization of the emitted pulse. We use a geometric description of the footprint area in each layer, i , as a function of time, t , from [11] for a pulse-limited altimeter

$$A_i(t) = \frac{\pi u_i t H}{1 + \frac{H}{R_e}} - \frac{\pi u_i (t - \tau) H}{1 + \frac{H}{R_e}} \quad (3)$$

where the second term is 0 when $t < \tau$. R_e is the Earth’s radius (6371 km), and u_i is the speed of light in the layer.

The backscattered energy, E , measured at the satellite for each model time-step (1×10^{-11} s), is the sum of the footprint area, A_i , multiplied by the layer backscatter coefficient, σ_i , i.e.,

$$E_t = \sum_{i=1}^n A_i \sigma_i. \quad (4)$$

The layer backscatter coefficient includes volume backscattering though its magnitude is negligible. The backscatter coefficient from each layer is adjusted for extinction using the radiative transfer approach, i.e.,

$$\sigma_i = (\sigma_i^{\text{surf}} + T_i^2 \sigma_i^{\text{vol.backs.}}) \prod_{i=1}^n \frac{1}{L_{i-1}^2} T_{i-1}^2. \quad (5)$$

L is the loss and T the transmission coefficient where $L_0 = T_0 = 1$ for the first layer. $\sigma_i^{\text{vol.backs.}}$ is the negligible volume backscatter coefficient. Surface scattering is synonymous with scattering at interfaces between layers such as the snow and ice surface or internal layers in the snow. Volume scattering is scattering from inclusions or particles within the layers, i.e., snow grains, voids, and air bubbles. The pulse propagation speed in snow and ice is a function of the layer permittivity (in Table I). Our model differs from an earlier altimeter waveform model, used for simulation of ice sheet signatures in [13], in its treatment of multiple scattering horizons and the more appropriate dense media volume scattering function. Further description of the forward model is given in [12].

III. FORWARD MODEL SIMULATION RESULTS

The snow and ice profile in Table I is taken as typical for the multiyear sea ice around the GreenIce camp in the Lincoln Sea, May 10–20, 2004. The camp was situated around 73°W ; 85°N , and the air temperatures were between -14°C and -6°C . The snow cover in the typical profile (Table I) is 25 cm, including 5-cm depth hoar immediately above the ice surface. The ice is 355 cm thick. The correlation length of the snow has been estimated according to its type using [14]. The flat-patch-area, a measure of roughness, has been estimated from altimeter observations between 0.2% and 16% for sea ice [1]. Here it has been set to 1% for both the snow and ice surface since there were no *in situ* measurements of this quantity. Its magnitude affects the simulated backscatter coefficient significantly but the effect on, e.g., half-power time is secondary to snow depth and density. In a sensitivity study where the snow and ice fractional flat-patch-area varies between 0.5% and 1.5%, the computed half-power time depth varies by 12 cm. At the same time the backscatter coefficient varies between realistic values of 22 and 27 dB. The range of backscatter values gives some justification for the range of flat-patch-area values in the sensitivity study. The half-power time is the point in time where the backscattered power received at the satellite reaches half its maximum. The half-power time is further converted to a depth beneath the snow surface, the effective scattering surface, by multiplying the speed of light in vacuum to simulate the apparent range variation.

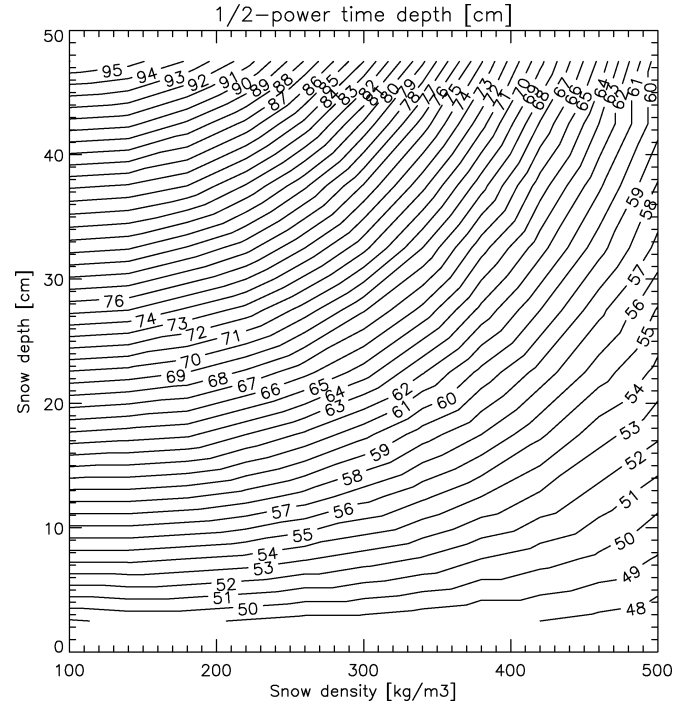


Fig. 1. Simulated half-power time depth beneath the snow surface (centimeters) as a function of snow density and snow depth. The simulated half-power time is multiplied by the speed of light in vacuum to illustrate the depth of the effective scattering surface. Only the snow density and the snow depth of the multiyear ice profile in Table I is varied.

Using the data of Table I as input to the model it is found that the simulated total backscatter coefficient of 25.6 dB is dominated (82%) by the ice surface scattering. The remaining 18% are scattered at the snow surface and volume backscattering in the snow and ice are negligible. The distribution of scattering magnitude between the snow and ice interface and the insignificant volume backscattering is consistent with measurements from [3]. The model is further used to simulate the influence of snow cover on the altimeter backscatter parameters that affect the altimeter elevation measurements. The effective scattering surface depth beneath the snow surface, shown in Fig. 1, is a function of both snow density between 100 and 500 kg/m^3 and snow thickness between 2.5 and 50 cm. Only these two snow parameters in the multiyear ice profile (Table I) are varied. The effective scattering surface depth is sensitive to snow depth because it decreases the total leading edge slope and thereby increases the half-power time as shown in Fig. 2. The backscattered energy is dominated first by snow surface scattering, then both snow and ice surface scattering. The point where the slope decreases is where the snow surface scattering is no longer increasing. Maximum backscattered energy is reached when ice surface scattering is no longer increasing. The different domains are marked by “snow,” “snow+ice,” and “ice” in the space beneath the curves in Fig. 2. The penetration depth, i.e., the depth where the transmitted unit power just beneath the surface has decreased to $1/e$, (in the above simulation it penetrates 30–80 cm below the snow surface) is also a function of both snow density and snow thickness. Fig. 3 shows a simulation of the resulting derived ice thickness using the range plus effective scattering surface depth and a constant reference over open water. The

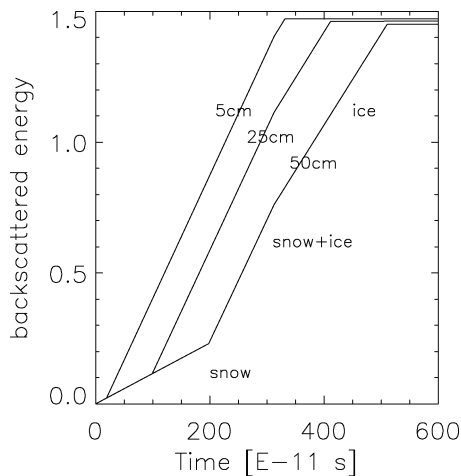


Fig. 2. Simulated leading edge of the multiyear ice pulse form for different snow cover depths. The curve to the left is for the 5-cm snow cover, the middle curve the 25-cm snow cover and the right curve the 50-cm snow cover. Except the snow depth all other parameters are similar to the multiyear ice profile in Table I.

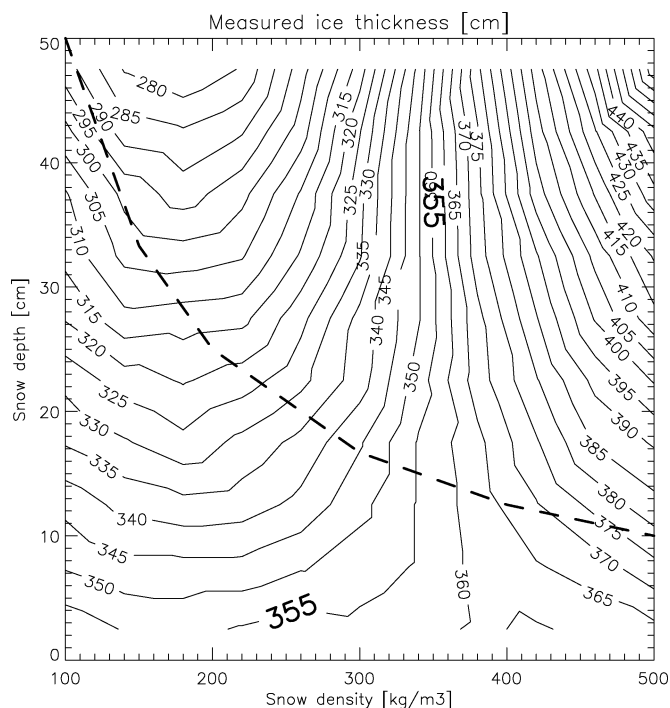


Fig. 3. Snow depth (centimeters) and density (kilograms per cubic meter) versus a simulation of measured ice thickness (centimeters) of a 355-cm-thick ice floe using ice half-power + range time and a water reference for different snow loads (the product of snow density and depth). The dashed line show a snow load of 50 kg/m^2 . In the simulation it is assumed that the ice freeboard is measured by the range + half-power time depth, this range measurement is compared to a “perfect” (constant) range measurement over water. The freeboard is then multiplied by 10 to obtain the simulated ice thickness measurement.

range is here the distance between the satellite and the snow surface. The range plus effective scattering surface depth is then the distance between the satellite and the effective scattering surface. The simulation includes the influence of the snow cover both on the ice floe buoyancy and the depth of the effective re-

flecting surface measured by the radar. The dashed line in Fig. 3 show a snow load of 50 kg/m^2 , i.e., where the ice surface is at constant height above the water. For this particular snow load the estimated ice thickness varies between 290 and 375 cm.

IV. CONCLUSION

Snow cover, i.e., snow depth and density, has a significant impact on the radar altimeter leading edge waveform. In particular, the snow depth increases the half-power time. The snow depth depresses the ice freeboard and elevates the snow surface. The simulated buoyant balance and the simulated radar ice elevation measurement counterbalance to some extent (extension of the radar range and elevation of the snow freeboard). However, the surface roughness, which is a secondary parameter for the effective scattering surface depth variation, can change without changing the floe buoyancy. It is, therefore, important also to quantify this parameter in future investigations. In order to proceed converting the apparent range measurement into estimates of sea ice freeboard and ice thickness, as proposed with CryoSat [15] and other Ku-band radar altimeters, systematic measurements of the snow cover are necessary. The estimated thickness of a 355-cm-thick floe with different snow covers, within the natural range of variability, varies between 325–405 cm at 25-cm snow depth and between 280–465 cm at 50-cm snow depth. For a constant snow load of 50 kg/m^2 (constant ice surface freeboard) the ice thickness estimate varies by 85 cm. Both the snow depth and density are important to lift the ambiguity. For example, the snow water equivalent (density times depth) often derived from microwave radiometer data is not sufficient.

It will further be impossible to distinguish snow and ice thickness anomalies using snow cover climatology and hemispheric sea ice snow mapping algorithms are therefore urgent if the prophecy of Rothrock should not become reality: “. . . to estimate the ice surface h_t [freeboard] and then multiply by . . . 10 to obtain thickness h introduces unsatisfactory errors” [16, p. 563].

ACKNOWLEDGMENT

Snow and ice profiles were collected by C. Haas.

REFERENCES

- [1] F. M. Fetterer, M. R. Drinkwater, K. C. Jezek, S. W. C. Laxon, R. G. Onstott, and L. M. H. Ulander, “Sea ice altimetry,” in *Microwave Remote Sensing of Sea Ice*, F. D. Carsey, Ed. Washington, DC: Amer. Geophys. Union, 1992, vol. 68, Geophysical Monograph, pp. 111–135.
- [2] M. Hallikainen and D. P. Winebrenner, “The physical basis for sea ice remote sensing,” in *Microwave Remote Sensing of Sea Ice*, F. D. Carsey, Ed. Washington, DC: Amer. Geophys. Union, 1992, vol. 68, Geophysical Monograph, pp. 29–46.
- [3] S. G. Beaven, G. L. Lockhart, S. P. Gogineni, A. R. Hosseinmostafa, K. Jezek, A. J. Gow, D. K. Perovich, A. K. Fung, and S. Tjuatja, “Laboratory measurements of radar backscatter from bare and snow-covered saline ice sheets,” *Int. J. Remote Sens.*, vol. 16, no. 5, pp. 851–876, 1995.
- [4] L. M. H. Ulander and A. Carlström, “Radar backscatter signatures of Baltic sea ice,” in *Proc. IGARSS*, 1991, pp. 1215–1218.
- [5] C. Mätzler, “Relation between grain-size and correlation length of snow,” *J. Glaciol.*, vol. 48, no. 162, pp. 461–466, 2002.
- [6] A. H. Sihvola and J. A. Kong, “Effective permittivity of dielectric mixtures,” *IEEE Trans. Geosci. Remote Sens.*, vol. 26, no. 4, pp. 420–429, Jul. 1988.

- [7] C. Mätzler, "Microwave properties of ice and snow," in *Solar System Ices*, B. Schmitt, Ed. *et al.* Dordrecht, The Netherlands: Kluwer, 1998, pp. 241–257.
- [8] M. E. Shokr, "Field observations and model calculations of dielectric properties of Arctic sea ice in the microwave C-band," *IEEE Trans. Geosci. Remote Sens.*, vol. 36, no. 2, pp. 463–478, Mar. 1998.
- [9] C. Mätzler and A. Wiesmann, "Extension of the microwave emission model of layered snowpacks to coarse-grained snow," *Remote Sens. Environ.*, vol. 70, pp. 317–325, 1998.
- [10] C. Mätzler, "Improved Born approximation for scattering of radiation in a granular medium," *J. Appl. Phys.*, vol. 83, pt. 11, pp. 6111–6117, 1998.
- [11] D. B. Chelton, J. C. Ries, B. J. Haines, L.-L. Fu, and P. S. Callahan, "Satellite altimetry," in *Satellite Altimetry and Earth Sciences*, L.-L. Fu and A. Cazenave, Eds. Orlando, FL: Academic, 2001.
- [12] R. Tonboe, S. Andersen, and L. T. Pedersen, "Sea ice radar altimeter signature modeling experiments," presented at the *1st CryoSat Workshop*, Mar. 8–10, 2005 [Online]. Available: <http://earth.esa.int/cryosat2005>.
- [13] J. K. Ridley and K. C. Partington, "A model of satellite radar altimeter return from ice sheets," *Int. J. Remote Sens.*, vol. 9, pp. 601–624, 1988.
- [14] A. Wiesmann, C. Mätzler, and T. Weise, "Radiometric and structural measurements of snow samples," *Radio Sci.*, vol. 33, no. 2, pp. 273–289, 1998.
- [15] D. Wingham, "The first of the European Space Agency's opportunity missions: CryoSat," *Earth Obs. Q.*, vol. 63, pp. 21–24, 1999.
- [16] D. A. Rothrock, "Ice thickness distribution—Measurement and theory," in *The Geophysics of Sea Ice*, ser. NATO ASI series, Series B: Physics N. Untersteiner, Ed. New York: Plenum, 1986, vol. 146, pp. 551–575.